Available online at www.medicinescience.org

ORIGINAL ARTICLE

Medicine Science International Medical Journal

Medicine Science 2026;15(2):707-12

Magnetic resonance imaging of Rosenmüller Fossa morphology in nasopharyngeal carcinoma

Mahmut Sabri Medisoglu[1], Melisa Ocbe[2]

[1]Kocaeli Health and Technology University, Faculty of Dentistry, Department of Anatomy, Kocaeli, Türkiye
[2]Kocaeli Health and Technology University, Faculty of Dentistry, Department of Oral and Maxillofacial Radiology, Kocaeli, Türkiye

Received 15 September 2025; Accepted 04 November 2025
Available online 27 April 2026 with doi: 10.5455/medscience.2025.09.246

Abstract

The Rosenmüller Fossa (RF) is the most common site of origin for nasopharyngeal carcinoma (NPC); however, its morphometric characteristics remain underinvestigated in clinical imaging studies. This study aimed to evaluate the morphological and dimensional differences in the RF between patients with NPC and healthy controls using magnetic resonance imaging (MRI). A retrospective analysis of MRI data from 41 patients with NPC and 49 age- and sex-matched controls without nasopharyngeal pathology was performed. Measurements included RF height, width, inter-fossa distance, and nasopharyngeal depth on axial and sagittal MR images. RF morphology was classified as Type A (shallow), Type B (deep and narrow), or Type C (deep and wide). The mean age of patients with NPC was 51.22 ± 13.81 years, and 68.29% were men. Tumor laterality was bilateral in 56.10% of the cases, and RF involvement was observed in 70.73% of the cases. No significant differences were found in right RF dimensions or R-L distance (p>0.05); however, left RF height was significantly reduced in patients with NPC (3.49 vs. 5.42 mm; p=0.013). Nasopharyngeal depth was also shorter in patients with NPC (17.40 mm vs. 19.03 mm; p=0.006). The RF morphology distribution did not differ significantly (p=0.381), although Type C fossae were more common in patients with NPC (26.83% vs. 14.29%). MRI revealed significant reductions in the left RF height and nasopharyngeal depth in patients with NPC, suggesting asymmetrical nasopharyngeal involvement. Detailed RF assessment using MRI may contribute to the early detection and improved staging of NPC.

Keywords: Rosenmüller fossa, recessus pharyngealis, nasopharyngeal carcinoma, magnetic resonance imaging

Introduction

The nasopharynx is a complex anatomical region at the skull base that plays a key role in respiration, swallowing, and auditory function [1,2]. The Rosenmüller Fossa (RF), also known as the lateral pharyngeal recess, is the most common site of origin for nasopharyngeal carcinoma (NPC) [3-7]. Early-stage NPC often arises submucosally within the RF, making it difficult to detect during routine clinical examinations. Therefore, radiological assessment of the RF is essential for the early diagnosis, staging, and treatment planning of NPC [7-13].

The morphological features of RF, including height, width, and depth, showed marked interindividual variation. Subtle changes, such as asymmetry or narrowing, may represent early tumor involvement, whereas anatomical differences can also mimic the disease and lead to diagnostic uncertainty. Therefore, an accurate morphometric evaluation of the RF is clinically relevant for detecting early NPC and distinguishing normal variants from pathological changes [14-16].

Previous studies have largely focused on RF anatomy using computed tomography (CT) and cone-beam CT (CBCT) [17-23]. These modalities provide high spatial resolution for osseous structures but have a limited ability to assess soft tissue changes that accompany NPC. Serindere et al. and Sutthiprapapaporn et al. proposed measurement protocols for RF morphometry on CT and CBCT images, respectively. However, the applicability of these methods to magnetic resonance imaging (MRI) has not been comprehensively explored [21,22]. Since MRI offers superior soft tissue contrast and is the imaging modality of choice for the local staging of NPC, applying morphometric assessment on MRI could enhance the radiological evaluation of RF.

CITATION
Medisoglu MS, Ocbe M. Magnetic resonance imaging of Rosenmüller Fossa morphology in nasopharyngeal carcinoma. Med Science. 2026;15(2):707-12.

OPEN ACCESS

Corresponding Author: Melisa Ocbe, Kocaeli Health and Technology University, Faculty of Dentistry, Department of Oral and Maxillofacial Radiology, Kocaeli, Türkiye
Email: melisa.ocbe@kocaelisaglik.edu.tr

DOI: 10.5455/medscience.2025.09.246

Despite the established role of MRI in nasopharyngeal imaging, few studies have systematically examined MRI RF morphology in patients with NPC compared to healthy controls [4,8,24,25]. Most previous studies have either described CT-based measurements or focused on general nasopharyngeal anatomy without addressing the RF as a distinct region [21-23,25]. Thus, the clinical significance of RF morphological characteristics on MRI remains unclear, and whether dimensional alterations correlate with the presence of NPC has not been adequately investigated.

Therefore, this study aimed to evaluate the morphological and dimensional characteristics of RF on MRI in patients with biopsy-proven NPC compared with those in age- and sex-matched controls. Specifically, we assessed whether RF dimensions (height, width, interfossa distance, and nasopharyngeal depth) and morphological classifications differed between the groups and whether such parameters may contribute to improved diagnostic interpretation in clinical practice.

Material and Methods

This retrospective study was approved by the Kocaeli Health and Technology University Non-Interventional Clinical Research Ethics Committee (No: 2025-128 Date: 10 March 2025) and conducted in accordance with the 1964 Declaration of Helsinki and its later amendments. Informed consent was waived due to the retrospective design.

Ninety MRI examinations performed between March 2022 and March 2024 were reviewed. After applying the eligibility criteria, 41 patients with biopsy-proven NPC and 49 controls without NPC were included. NPC group (n=41): Patients with no history of surgery or radiotherapy before imaging. The exclusion criteria were congenital anomalies, prior head and neck surgery, radiotherapy, and poor image quality due to motion artifacts. Control group (n=49): Controls were selected from individuals who underwent MRI for unrelated complaints (e.g., headache, sinus evaluation, and nonspecific symptoms) but were confirmed to have no evidence of nasopharyngeal pathology. Patients with suboptimal image quality or a history of sinonasal or nasopharyngeal surgery were excluded from the study. The NPC group consisted of 28 men (68.29%) and 13 women (31.71%) with a mean age of 51.22 ± 13.81 years, while the control group included 24 men (48.98%) and 25 women (51.02%) with a mean age of 53.14 ± 25.09 years.

All MRI examinations were performed using a 3T scanner (SIGNA™ Pioneer, GE Medical Systems, Waukesha, WI, USA) with a dedicated head-and-neck coil. All morphometric measurements were performed by a single observer, an oral and maxillofacial radiologist with 8 years of experience in interpreting MRI and CT scans of the head and neck. Axial, sagittal, and coronal sequences were acquired, including T1-weighted, T2-weighted fast spin-echo (FSE), short tau inversion recovery (STIR), and LAVA-Flex (T1 Dixon-based gradient echo) images. T1-weighted and LAVA-Flex images provided high-resolution anatomical details and delineation of the RF boundaries relative to the adjacent musculature and fat planes. T2-weighted FSE and STIR sequences were used to assess soft tissue contrast and detect mucosal thickening or submucosal infiltration that could influence the appearance or depth of the RF. In addition to morphometric measurements, a qualitative assessment of the signal intensity within the RF was performed to ensure proper anatomical identification. In normal cases, the RF exhibits an intermediate signal intensity on T1-weighted images and a hyperintense appearance on T2-weighted and STIR sequences. The hyperintense imaging characteristics are due to the mucosal lining and retained air or secretions within the recess. In patients with NPC, focal or diffuse signal intensity alterations (e.g., intermediate-to-low on T1 and intermediate-to-high on T2/STIR) were noted when tumor infiltration or mucosal thickening was suspected.

Morphometric and Classification Parameters

Measurements were performed on axial and sagittal MR images using the reference points described in previous CBCT-based studies, which were adapted for MRI visualization. To avoid confusion, the following terminology was consistently applied [21-23] (Figure 1).

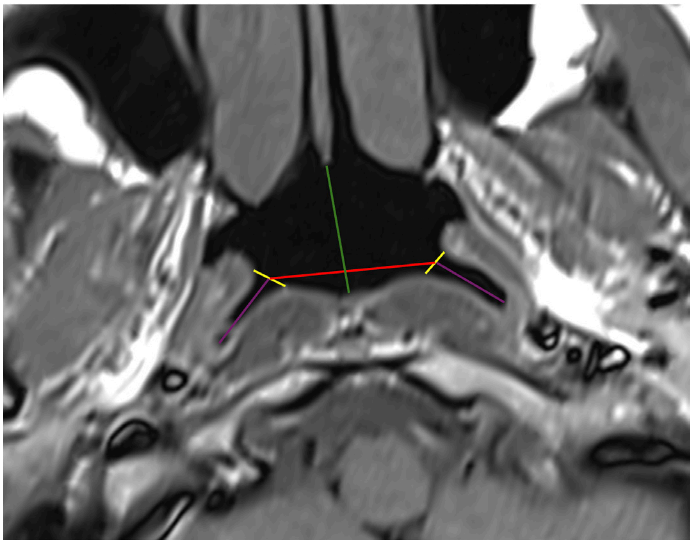

Figure 1. T1-weighted FSE MR image depicting morphometric measurements of the Rosenmüller Fossa (RF) and its anatomical relationship with surrounding structures. Yellow lines indicate the bilateral openings of the RF. Purple lines represent the depth of the RF on both sides. The red line measures the transverse distance between the right and left RF. The green line shows the linear distance between the posterior nasal spine (PNS) and posterior pharyngeal wall, serving as a reference for nasopharyngeal depth

1. **Rosenmüller Fossa (RF) Opening Width:** This measurement was performed bilaterally on the axial MR images. It was defined as the linear distance between the anterior and posterior borders of the RF. The anterior border was identified at the posterior margin of the Eustachian tube orifice, and the posterior border corresponded to the beginning of the lateral pharyngeal recess.

 DOI: 10.5455/medscience.2025.09.246

2. **Rosenmüller Fossa (RF) Depth:** The RF depth was measured as the maximum perpendicular distance from a straight line drawn between the anterior and posterior margins of the RF opening to the deepest point of the fossa. This measurement reflects the lateral extension of the fossa into the pharyngeal wall and is performed bilaterally.
3. **Interfossa Distance:** This transverse measurement was obtained by drawing a horizontal line between the deepest points of the right and left Rosenmüller Fossa on an axial slice that included both structures at their maximum depth. This value reflects the total transverse span of the nasopharynx at the fossa level.
4. **Nasopharyngeal Depth:** Nasopharyngeal depth was measured in the midsagittal plane. It was defined as the linear distance from the posterior nasal spine (PNS) to the posterior pharyngeal wall. The PNS was identified as the pointed posterior projection of the hard palate, and the posterior wall was defined as the mucosal interface adjacent to the prevertebral space. This measurement reflects the anteroposterior width of the nasopharynx of the patient.

The morphology of the RF was classified according to the study by Keskek [23]. Based on the previously established classification criteria, each RF was categorized into one of three morphological types according to its depth and width, as measured on axial MR images:

Type A: Characterized by a shallow fossa with a depth of<5 mm. This type is considered anatomically less prominent and is typically observed in individuals without significant lateral pharyngeal recess formation. It may be challenging to differentiate in cases with mucosal thickening or poor soft tissue contrast (Figure 2A).

Type B: Defined by a depth equal to or greater than 5 mm but with a width of less than 1 mm. This configuration indicates a deeper but narrower fossa, often appearing as a slender, slit-like extension into the lateral pharyngeal wall. Type B morphology may still be difficult to detect if the lateral extension is obscured by adjacent soft tissue structures (Figure 2B).

Type C: Identified when the RF had a depth of ≥5 mm and a width of ≥1 mm. This is the most prominent form, showing a wide and deep recess extending laterally and posteriorly. Type C fossae are typically more easily visualized on axial MR images and are often observed in patients with increased susceptibility to nasopharyngeal pathologies. These classifications were applied bilaterally for each patient, and both sides were independently evaluated (Figure 2C).

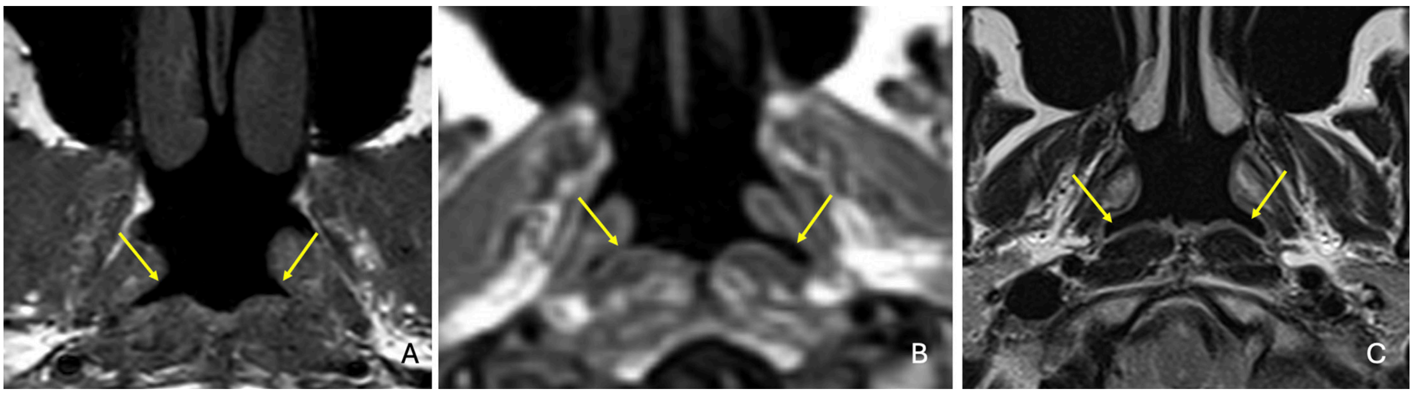

Figure 2. Axial MR images demonstrating the morphological classification of the Rosenmüller Fossa (RF). A. Axial T1-weighted FSE image illustrating Type A RF, characterized by a shallow recess with a depth of less than 5 mm. B. Axial T1-weighted FSE image showing Type B RF, defined by a depth equal to or greater than 5 mm and a narrow width less than 1 mm. C. Axial T2-weighted FSE image depicting Type C RF, with a depth greater than 5 mm and a width equal to or exceeding 1 mm, indicating a prominent and well-developed fossa

All measurements were performed using digital calipers on the PACS system. When bilateral structures were evaluated, measurements were performed on both sides. If asymmetry was noted, the side with greater involvement (in NPC cases) or the more prominent anatomical dimension (in the controls) was recorded for analysis. Slice selection was standardized, and the axial slice demonstrating the maximum RF depth was chosen for each side. In cases in which the RF appeared closed (opposing mucosal walls in contact), the fossa depth was recorded as 0 mm and included in the statistical analysis.

The categorical variables were sex and RF classification (Type A, shallow fossa <5 mm; Type B, deep fossa ≥5 mm; and Type C, deep fossa with wide openings >1 mm). The continuous variables were age, RF height and width measurements on both sides, R-L distance, and distance between the PNS and posterior wall of the nasopharynx. Statistical analyses were conducted using the Python 3.11, SciPy, and Pandas libraries. The normal distribution of continuous variables was assessed using the Shapiro–Wilk test. Differences in continuous variables between the control and NPC groups were analyzed using Welch's t-test. For categorical data, particularly the distribution of RF morphological types, the chi-square test of independence was used to assess whether there was a statistically significant association between RF type and NPC. Effect sizes were also calculated to complement statistical

DOI: 10.5455/medscience.2025.09.246

significance, with Cohen's d reported for t-tests and Cramér's V for the chi-square test. Statistical significance was set at p<0.05. Intraobserver reliability was assessed in a randomly selected subset of 12 cases using the intraclass correlation coefficient (ICC) in a two-way mixed-effects model (absolute agreement). The same observer repeated the measurements for this subset at two different time points under identical imaging conditions. The variables measured included the height and width of the right and left RFs and the right–left distance.

Results

The study included 41 patients with NPC and 49 controls. The mean age of the NPC group was 51.22 years (SD=13.81), with a median of 56.00 years and a range of 21–75 years. Among these patients, 13 (31.71%) were women and 28 (68.29%) were men (Table 1). Regarding tumor laterality, 10 (24.39%) presented with right-sided involvement, 8 (19.51%) with left-sided involvement, and 23 (56.10%) with bilateral NPC (Table 2). Radiological evaluation revealed RF involvement in 29 patients (70.73%), whereas no involvement was observed in the remaining 12 patients (29.27%).

Table 1. Demographic characteristics of the study population

Parameters	NPC group (n=41)	Control group (n=49)	p-value
Age (mean ± SD)	51.22 ± 13.81	53.14 ± 25.09	
Gender - Female, n (%)	13 (31.71)	25 (51.02)	0.65
Gender - Male, n (%)	28 (68.29)	24 (48.98)	

Continuous variables were compared using Welch's t-test, and categorical variables were compared using the chi-squared test. Statistical significance was set at p<0.05

Table 2. Tumor laterality and Rosenmüller Fossa involvement (NPC Group)

Tumor side	n (%)
Right	10 (24.39)
Left	8 (19.51)
Bilateral	23 (56.10)
RF involvement	29 (70.73)
No RF involvement	12 (29.27)

Descriptive data are presented as frequencies and percentages. No statistical comparisons were performed because the data represent subgroup characteristics within the NPC group

Dimensional analysis of the RF in the NPC group showed that the mean height and width of the right RF were 4.41 mm (SD=3.51) and 4.01 mm (SD=3.08 mm), respectively. On the left side, the mean height was 3.49 mm (SD=3.17), and the mean width was 3.97 mm (SD=2.55). The distance between the right and left fossae had a mean value of 17.47 mm (SD=4.63), while the mean distance to the PNS was 17.40 mm (SD=4.34) (Table 3).

Table 3. Morphometric measurements of the Rosenmüller Fossa

Measurement	NPC (mean ± SD)	Control (mean ± SD)	p-value
Right RF height	4.41 ± 3.51	4.19 ± 3.21	0.76
Right RF width	4.01 ± 3.08	3.21 ± 1.33	0.13
Left RF height	3.49 ± 3.17	5.42 ± 4.03	0.013*
Left RF width	3.97 ± 2.55	3.52 ± 1.60	0.33
R-L distance	17.47 ± 4.63	17.82 ± 3.65	0.70
PNS to posterior wall of nasopharynx	17.40 ± 4.34	19.03 ± 4.48	0.006*

Group comparisons were performed using Welch's t-test. Statistical significance was set at p<0.05; significant differences are indicated by an asterisk (*)

The morphological classification of the RF in the NPC group revealed that most patients (63.41%) exhibited Type A morphology (shallow fossa<5 mm). Type B (deep fossa ≥ 5 mm) was observed in 9.76% of cases, whereas Type C (deep and wide fossa) was present in 26.83% of cases (Table 4).

Table 4. Distribution of Rosenmüller Fossa morphological types

RF type	NPC group	Control group	p-value
Type A	26 (63.41%)	33 (67.35%)	
Type B	4 (9.76%)	9 (18.37%)	0.381
Type C	11 (26.83%)	7 (14.29%)	

The distribution of Rosenmüller Fossa types between the groups was compared using the chi-squared test of independence. Statistical significance was set at p<0.05

In the control group, the mean age was 53.14 years (SD=25.09), with a median of 50.00 years and a range of 19–92 years. Of the 49 individuals in the control group, 25 (51.02%) were women and 24 (48.98%) were men. The RF measurements in the control group indicated a mean right RF height of 4.19 mm (SD=3.21) and a width of 3.21 mm (SD=1.33). The left RF showed a mean height of 5.42 mm (SD=4.03) and a mean width of 3.52 mm (SD=1.60). The distance between the right and left fossae was 17.82 mm (SD=3.65), and the mean PNS distance was 19.03 mm (SD=4.48). Morphological classification in the control group showed a predominance of Type A (67.35%), followed by Type B (18.37%), and Type C (14.29%).

A statistical comparison between the NPC and control groups using independent samples t-tests revealed no significant differences in age (p=0.65), right RF height (p=0.76), right RF width (p=0.13), left RF width (p=0.33), distance between the right and left fossae (p=0.70), or PNS (p=0.006). However, a statistically significant difference in the height of the left RF was observed (p=0.013), with lower values in the NPC group.

DOI: 10.5455/medscience.2025.09.246

Additionally, the PNS distance was significantly shorter in the NPC group (p=0.006). A chi-square analysis evaluating the association between RF morphological types (A, B, and C) and group classification (NPC vs. control) did not reveal a statistically significant relationship (p=0.381). An intraobserver reliability analysis demonstrated an ICC of 0.92, reflecting excellent agreement between repeated measurements.

Discussion

This study evaluated the morphological and dimensional characteristics of RF on MRI in patients with NPC compared to healthy controls. To the best of our knowledge, this is the first systematic investigation of RF morphometry using MRI. This imaging modality provides superior soft-tissue contrast and is routinely used for NPC staging.

Our results demonstrated that the left RF height was significantly lower in patients with NPC than in controls (p=0.013). This finding suggests that tumor-related invasion, inflammation, or regional fibrosis may contribute to the asymmetrical narrowing of the fossa. Previous CT-based studies have reported that early NPC often presents as asymmetry or blunting of the RF rather than as a distinct mass, reflecting submucosal tumor spread [21,22]. Current MRI-based evidence supports this concept by quantitatively documenting dimensional reduction in affected patients. In addition, the nasopharyngeal depth (PNS; posterior wall distance) was significantly shorter in the NPC group (p=0.006), consistent with potential posterior wall compression or tumor infiltration, as described in radiological reports of early NPC involvement.

Although the distribution of morphological RF types (A–C) did not differ significantly between the groups, we observed a greater frequency of Type C (deep and wide) fossae among patients with NPC (26.83% vs. 14.29%). Although not statistically significant, this observation raises the possibility that larger and deeper fossae may be predisposed to tumor development or more easily infiltrated. While Type C morphology (deep and wide fossa) has been suggested to occur more frequently in NPC cases, the longer mean left RF length observed in the control group may initially seem counterintuitive. However, it should be considered that Type B morphology also represents a deep fossa, differing from Type C primarily in terms of its narrower width. Consequently, the presence of Type B fossae among the control subjects could explain the greater mean depth without implying pathological enlargement. This highlights the need to evaluate both depth and width parameters collectively rather than in isolation when interpreting RF morphology. Previous studies have shown that RF size and shape vary with adenoid tissue distribution, prevertebral muscle structure, and age-related changes [25,26]. Age-related changes, such as mucosal thinning, regression of adenoid tissue, and decreased muscular tone, can alter the depth and width of the fossa. Similarly, sex-related anatomical differences in craniofacial dimensions and nasopharyngeal volume may contribute to the variability in RF measurements [25,26]. Although our study groups were matched for age and sex, these factors could still account for some of the interindividual variations observed and should be considered in future research. In the present study, although age matching was achieved between groups, a higher proportion of male patients was observed in the NPC group, consistent with the recognized male predominance in NPC. This imbalance may have introduced a minor confounding effect, as sexual dimorphism in the craniofacial anatomy can influence the nasopharyngeal dimensions and RF morphology. However, previous morphometric studies have shown that these variations are generally subtle and are unlikely to alter the diagnostic implications of the current findings. Future studies with strictly balanced sex distributions could help further validate these observations. Our findings are consistent with the view that RF morphology demonstrates considerable interindividual variation, and while dimensional reduction may indicate tumor involvement, baseline variability must be considered during radiological interpretation.

Our measurement approach adapted the CBCT-based methods described by Serindere et al. and Sutthiprapaporn et al. for MRI assessment [21,22]. These earlier studies defined standardized landmarks for RF morphometry but primarily assessed bony boundaries. In contrast, MRI enables a more precise evaluation of soft-tissue structures and submucosal changes, which are crucial for the early detection of NPC. Similar to previous CT reports [18-23,25], our study confirmed that the dimensional asymmetry of the RF is a key indicator of pathological involvement. Importantly, we found that these alterations can be quantified using MRI, reinforcing its diagnostic utility in this anatomical region.

This study has several limitations that must be acknowledged. First, this was a retrospective study conducted at a single institution with a relatively modest sample size, which may limit its generalizability. Second, T-staging data were not uniformly available, preventing a correlation between RF morphology and tumor stage. Previous studies using CT acquired in the upright position have demonstrated differences in RF dimensions according to posture. This factor should be considered in future comparative studies. Finally, this study focused primarily on the morphometric assessment of the RF rather than on the quantitative analysis of its signal intensity characteristics. Although qualitative differences in intensity were observed between normal and pathological cases, standardized quantitative methods (e.g., region-of-interest (ROI)-based signal intensity measurements or contrast-to-noise ratio analysis) were not applied. Future studies using objective signal quantification across multiple MRI sequences may provide deeper insights into tissue composition, early tumor infiltration, and the diagnostic value of MRI intensity mapping in nasopharyngeal evaluation.

DOI: 10.5455/medscience.2025.09.246

Conclusion

This MRI-based study demonstrated that patients with NPC exhibited significant reductions in left RF height and nasopharyngeal depth compared to healthy controls. Although RF morphological type alone was not predictive of NPC, dimensional asymmetry may serve as an early radiological marker of tumor involvement. These findings highlight the clinical relevance of detailed RF evaluation on MRI and support its incorporation into routine nasopharyngeal imaging. Future research with larger multicenter cohorts and the integration of tumor staging is warranted to further validate the diagnostic significance of RF morphometry.

Ethical Approval
Approved by the Kocaeli Health and Technology University Non-Interventional Research Ethics Committee (No: 2025-128; Date: 10 March 2025).

Patient Consent
Informed consent was waived due to the retrospective design.

Conflict of Interest
The authors declare no conflict of interest.

Funding
The authors received no financial support for this study.

References

1. Tisza VB, Gumpertz E. The parents' reaction to the birth and early care of children with cleft palate. Pediatrics. 1962;30:86–90.
2. Chong VFH, Ong CK. Nasopharyngeal carcinoma. Eur J Radiol. 2008;66:437–47.
3. Chong VFH, Fan YF. Radiology of the masticator space. Clin Radiol. 1996;51:457–65.
4. Goh J, Lim K. Imaging of nasopharyngeal carcinoma. Ann Acad Med Singapore. 2009;38:809–16.
5. Amene C, Cosetti M, Ambekar S, et al. Johann Christian Rosenmüller (1771–1820): A historical perspective on the man behind the fossa. J Neurol Surg B Skull Base. 2013;74:187–93.
6. Smith ME, Scoffings DJ, Tysome JR. Imaging of the Eustachian tube and its function: A systematic review. Neuroradiology. 2016;58:543–56.
7. Sakata K, Hareyama M, Tamakawa M, et al. Prognostic factors of nasopharynx tumors investigated by MR imaging and the value of MR imaging in the newly published TNM staging. Int J Radiat Oncol Biol Phys. 1999;43:273.
8. Zhang F, Sha Y. Computed tomography and magnetic resonance imaging findings for primary middle-ear carcinoma. J Laryngol Otol. 2013;127:578–83.
9. Miyahara H, Matsunaga T. Tornwaldt's disease. Acta Otolaryngol Suppl. 1994;114:36–39.
10. Velayutham P, Davis P, Savery N, Vaigundavasan R. A common symptom with an uncommon diagnosis. Egypt J Otolaryngol. 2021;37:95.
11. Bergin M, Bird P, Cowan I, Pearson JF. Exploring the critical distance and position relationships between the Eustachian tube and the internal carotid artery. Otol Neurotol. 2010;31:1511–15.
12. Gibb GA. Nasopharyngeal Carcinoma. 2nd ed. The Chinese University of Hong Kong. 1999:19–21.
13. Tobias PV. The nasopharynx: review of structure and development, with notes on speech, pharyngeal hypophysis, chordoma and the dens. J Dent Assoc S Afr. 1981;36:765–78.
14. O'Rahilly R, Müller F. Human Embryology and Teratology. 3rd ed. New York: Wiley-Liss. 2001:242–49.
15. Davis KR. Embolization of epistaxis and juvenile nasopharyngeal angiofibromas. AJR Am J Roentgenol. 1987;148:209–18.
16. Arıncı K, Elhan A. Anatomi. 3rd edition. İstanbul: Güneş Kitabevi. 2001.
17. Kaplan FA, Saglam H, Bilgir E, Bayrakdar IS, Orhan K. Radiological evaluation of the recesses on the posterior wall of the nasopharynx with cone-beam computed tomography. Niger J Clin Pract. 2022;25:55–61.
18. Takasugi Y, Futagawa K, Konishi T, Morimoto D, Okuda T. Possible association between successful intubation via the right nostril and anatomical variations of the nasopharynx during nasotracheal intubation: a multiplanar imaging study. J Anesth. 2016;30:987–93.
19. Temiz M, Duman SB, Abdelkarim AZ, et al. Nasopharynx evaluation in children of unilateral cleft palate patients and normal with cone beam computed tomography. Sci Prog. 2023;106:368504231157146.
20. Duggappa AKH, Mathew S, Gupta DN, et al. Comparison of nasopharyngeal temperature measured at fossa of Rosenmuller and blindly inserted temperature probe with esophageal temperature. Anesth Essays Res. 2018;12:506–11.
21. Serindere G, Gunduz K, Avsever H, Orhan K. The anatomical and measurement study of Rosenmüller Fossa and oropharyngeal structures using cone beam computed tomography. Acta Clin Croat. 2022;61:177–84.
22. Sutthiprapaporn P, Tanimoto K, Ohtsuka M, et al. Improved inspection of the lateral pharyngeal recess using cone-beam computed tomography in the upright position. Oral Radiol. 2008;24:71–75.
23. Erdem Ş, Zengin AZ, Erdem Ş. Evaluation of the pharyngeal recess with cone-beam computed tomography. Surg Radiol Anat. 2020;42:1307–13.
24. Kusaka T, Kuwashima S, Hiraumi H, Sato H. A case of actinomycosis in the Rosenmüller's fossa. Ear Nose Throat J. 2022;101:NP389–NP391.
25. Hoe J. CT of nasopharyngeal carcinoma: significance of widening of the preoccipital soft tissue on axial scans. AJNR Am J Neuroradiol. 1989;10:839–44.
26. Mancuso AA, Bohman LG, Hanafee WN, et al. Computed tomography of the nasopharynx: normal and variants of normal radiology. Radiology. 1980;137:113–21.